

Cobalt Chemistry with Mixed Aminotroponimate Salicylaldimine Ligands: Synthesis, Characterization, and Nitric Oxide Reactivity

Scott A. Hilderbrand and Stephen J. Lippard*

Department of Chemistry, Massachusetts Institute of Technology, Cambridge, Massachusetts 02139

Received February 18, 2004

A new class of mixed aminotroponimine salicylaldimine ligands and their corresponding cobalt(II) complexes are reported. This work expands the family of cobalt(II) aminotroponimate complexes to include salicylaldimine and derivatized fluorescein moieties. The $H_2^{iPr}SATI-n$ ($n = 3, 4$) ligands **3** and **4**, respectively, contain an aminotroponimine moiety and a salicylaldimine fragment connected with an alkyl linker. In the $H_2^{iPr}FATI-n$ ($n = 3, 4$) ligands **5** and **6**, a derivatized fluorescein replaces the salicylaldimine fragment. The cobalt(II) complexes $[Co^{(iPr)SATI-3}]$ (**7**) and $[Co_2^{(iPr)SATI-4}]$ (**9**) were prepared and structurally characterized. The reaction of NO with both complexes ultimately results in the formation of a dinitrogen-containing species. The mononitrosyl, $[Co^{(iPr)SATI-3}(NO)]$ (**8**), was isolated and characterized. The reactivity of $[Co^{(iPr)FATI-3}]$ (**10**) and $[Co^{(iPr)FATI-4}]$ (**11**) with NO mimics that observed for the salicylaldimine derivatives, as monitored by solution IR spectroscopy. When followed by fluorescence spectroscopy, reaction of **11** with NO evoked a 3-fold increase in emission intensity after 22 h.

Introduction

Nitric oxide, a diatomic gas having one unpaired electron in its antibonding π^* molecular orbital, is the subject of intensive study. Traditionally, research has focused on the roles of NO in the troposphere as an environmental pollutant. In the 1980s, however, NO was discovered to have important physiological functions.^{1–4} Nitric oxide is a ubiquitous biological messenger, playing key roles in the cardiovascular, immune, and nervous systems.^{4–12} It reacts readily with a variety of species commonly found in biological systems

such as dioxygen, oxygen radicals, thiols, amines, and transition metals.¹³ These reactions form N_2O , NO^+ , N_2O_4 , *S*-nitrosothiols, *N*-nitrosamines, and metal–nitrosyl complexes. Many of these products are more reactive than NO itself. Strategies to detect NO in biological settings have become increasingly more sophisticated, as reviewed elsewhere.¹⁴

One highly sensitive method for imaging biological NO is based on fluorescence detection. In recent studies of the chemistry of nitric oxide with $[Co(DATI-4)]$ and related compounds, a design strategy evolved for a fluorescence-based NO sensor, as described in Scheme 1. Upon reaction with excess NO, both $[Co^{(iPr)DATI}_2]$ and $[Co^{(iPr)DATI-4}]$ complexes exhibit a steady increase in fluorescence emission intensity over several hours that is attributed to ejection of one of the dansyl moieties from the cobalt coordination sphere.¹⁵ These reactions are too slow for use in biological systems, however, and neither complex is water-soluble. Moreover, the relatively high excitation energy of the dansyl group is not ideal for the optical imaging of NO in vivo.

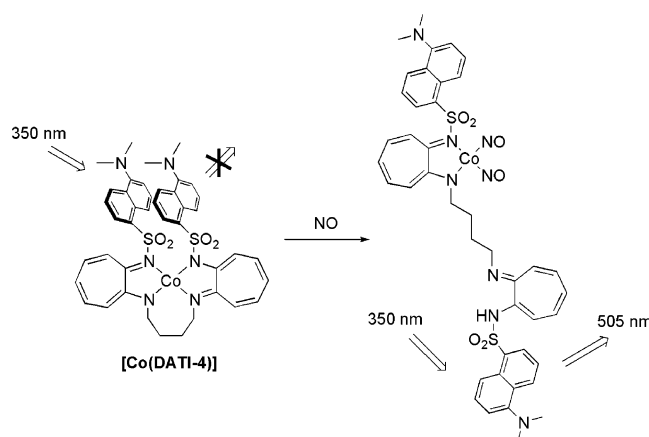
In pursuit of improved reagents to detect NO rapidly with the use of fluorescence spectroscopy and transition metal–

* To whom correspondence should be addressed. E-mail: lippard@lippard.mit.edu.

- (1) Palmer, R. M. J.; Ferrige, A. G.; Moncada, S. *Nature* **1987**, *327*, 524–526.
- (2) Furchgott, R. F. *Angew. Chem., Int. Ed.* **1999**, *38*, 1870–1880.
- (3) Ignarro, L. J.; Buga, G. M.; Wood, K. S.; Byrns, R. E.; Chaudhuri, G. *Proc. Natl. Acad. Sci. U.S.A.* **1987**, *84*, 9265–9269.
- (4) Ignarro, L. J. *Angew. Chem., Int. Ed.* **1999**, *38*, 1882–1892.
- (5) Wink, D. A.; Vodovotz, Y.; Laval, J.; Laval, F.; Dewhirst, M. W.; Mitchell, J. B. *Carcinogenesis* **1998**, *19*, 711–721.
- (6) Moncada, S.; Palmer, R. M. J.; Higgs, E. A. *Pharmacol. Rev.* **1991**, *43*, 109–142.
- (7) Kerwin, J. F., Jr.; Lancaster, J. R., Jr.; Feldman, P. L. *J. Med. Chem.* **1995**, *38*, 4343–4362.
- (8) Feldman, P. L.; Griffith, O. W.; Stuehr, D. J. *Chem. Eng. News* **1993**, *71*, 26–38.
- (9) Brecht, D. S.; Snyder, S. H. *Annu. Rev. Biochem.* **1994**, *63*, 175–195.
- (10) Murad, F. *Angew. Chem., Int. Ed.* **1999**, *38*, 1856–1868.
- (11) Butler, A. R.; Williams, D. L. H. *Chem. Soc. Rev.* **1993**, *22*, 233–241.
- (12) Rubbo, H.; Darley-Usmar, V.; Freeman, B. A. *Chem. Res. Toxicol.* **1996**, *9*, 809–820.

- (13) Pfeiffer, S.; Mayer, B.; Hemmens, B. *Angew. Chem., Int. Ed.* **1999**, *38*, 1714–1731.
- (14) Nagano, T.; Yoshimura, T. *Chem. Rev.* **2002**, *102*, 1235–1269.
- (15) Franz, K. J.; Singh, N.; Spingler, B.; Lippard, S. J. *Inorg. Chem.* **2000**, *39*, 4081–4092.

Scheme 1



nitrosyl chemistry, we have investigated a number of different tactical approaches. The use of rhodium-based systems addresses several of the issues, as reported elsewhere.¹⁶ The aim of the present work was to obtain complexes that achieve water solubility utilizing a fluorophore with longer wavelength excitation and emission bands than the dansyl moieties used in the DATI complexes. To achieve these goals, we designed a family of Co(II) complexes with ligands containing an aminotroponimate moiety linked to a derivatized fluorescein having a coordination mode similar to that of a salicylaldiminate group. Fluorescein has optical properties that are more amenable to biological sensing than the dansyl group employed in the DATI complexes. It typically has high quantum yields, approaching unity, and long wavelength excitation of 490 nm or greater. In addition, since fluorescein is more polar than dansyl, complexes with fluorescein-containing ligands usually convey better water solubility. Owing to difficulties in the purification and the preparation of large quantities of the fluorescein-containing complexes for structural characterization, salicylaldiminate analogues were prepared for comparison purposes and to investigate their NO reactivity.

Although our initial objectives were accomplished, the reactivity of the ⁱPrFATI-*n* and ⁱPrSATI-*n* Co(II) complexes with NO proved to be complex, leading us to pursue other tactics for detecting biological NO by fluorescence using transition metal scaffolds.¹⁶ Nevertheless, the new class of mixed ligands containing an aminotroponimate and salicylaldiminate or salicylaldiminate-like fragment allowed us to explore some interesting cobalt coordination chemistry. The details of these studies comprise the present report.

Experimental Section

General Considerations. Pentane, tetrahydrofuran (THF), and diethyl ether (Et₂O) were purified by passage through alumina columns under a N₂ atmosphere.¹⁷ Dichloromethane (CH₂Cl₂), chloroform (CHCl₃), and acetonitrile (CH₃CN) were distilled from CaH₂ under a N₂ atmosphere. Anhydrous dimethyl sulfoxide (DMSO), packaged under N₂, was purchased from Aldrich and used

as received. Methanol (MeOH) used for fluorescence studies was distilled from magnesium and iodine under a N₂ atmosphere. All other solvents were purchased from Mallinckrodt or EM Science and used without further purification. Silica gel 60 (230–400 mesh, EM Science) was used for column chromatography. The starting materials, 2-(isopropylamino)troponone,¹⁸ and 7'-chloro-4'-fluoresceincarboxaldehyde¹⁹ were prepared as previously described. All other reagents were obtained commercially and used without further purification. IR spectra were recorded on a Bio Rad FTS-135 or a Thermo Nicolet AVATAR 360 spectrophotometer. In situ IR spectra were recorded on a ReactIR 1000 instrument from ASI equipped with a 1-in.-diameter, 30-reflection silicon ATR (SiComp) probe. UV–vis spectra were recorded on a Hewlett-Packard 8435 spectrophotometer. Unless otherwise mentioned, fluorescence emission intensity spectra were recorded at 25 ± 0.2 °C on a Hitachi F-3010 fluorescence spectrophotometer. Electrospray ionization (ESI) mass spectrometry was performed in the MIT Department of Chemistry Instrumentation Facility. APCI mass spectrometric data were acquired on an Agilent 1100 MSD system. NMR spectra were recorded on a Bruker DPX-400 spectrometer at ambient temperature and referenced to internal ¹H and ¹³C solvent peaks. Nitric oxide (Matheson 99%) was purified by a method adapted from the literature.²⁰ The NO stream was passed through an Ascarite (NaOH fused on silica gel column and a 6 ft coil filled with silica gel cooled to –78 °C with a dry ice/acetone bath).

N-(3-Amino(*n*-propylamino)-2-(isopropylamino)troponimine (1). Under an atmosphere of argon, finely divided Me₃OBF₄ (2.66 g, 18.0 mmol) was added to a solution of 2-(isopropylamino)troponone (2.00 g, 12.2 mmol) in 30 mL of CH₂Cl₂ and allowed to stir for 2 h. The golden-yellow solution was added dropwise to neat 1,3-diaminopropane (15 mL, 180 mmol) over 45 min and allowed to stir for 2 h. After quenching with 40 mL of water, the aqueous layer was extracted with CH₂Cl₂ (3 × 25 mL). The organic extracts were dried over MgSO₄ and filtered, and the solvent was removed under reduced pressure giving a brown-yellow oil. The crude material was dissolved in dilute aqueous HCl. The solution was first extracted with CH₂Cl₂ to remove unwanted byproducts. The pH of the solution was then raised to 9 with aqueous NaOH, and further extraction with CH₂Cl₂ (3 × 75 mL) was performed. The organic extract was dried over MgSO₄ and filtered, and the solvent was removed under reduced pressure giving **5** (880 mg, 33%) as a yellow oil. ¹H NMR (400 MHz, CD₂Cl₂): δ 6.74–6.70 (2H, m), 6.33 (1H, d, *J* = 11.3 Hz), 6.25 (1H, d, *J* = 10.9 Hz), 6.13–6.08 (1H, m), 3.82 (1H, septet, *J* = 6.3 Hz), 3.36 (2H, t, *J* = 6.8 Hz), 2.82 (2H, t, *J* = 6.8 Hz), 1.84 (2H, p, *J* = 6.8 Hz), 1.23 (6H, d, *J* = 6.3 Hz). ¹³C NMR (100 MHz, CDCl₃): δ 153.44, 151.08, 133.14, 132.58, 117.42, 112.39, 107.76, 44.99, 40.57, 34.13, 22.72. IR (NaCl, cm⁻¹): 3212 (w br), 2964 (m), 2928 (m), 2863 (w), 1589 (m), 1536 (m), 1510 (m), 1463 (m), 1414 (w), 1384 (m), 1326 (w), 1303 (w), 1272 (m), 1232 (w), 1206 (w), 1167 (m), 1121 (m br), 976 (w), 951 (w), 882 (w), 864 (w), 844 (w), 817 (w), 746 (w), 704 (m), 636 (w br). HRMS (ESI) MH⁺: calcd for C₁₃H₂₂N₃, 220.1814; found, 220.1802.

N-(4-Amino(*n*-butylamino))-2-(isopropylamino)troponimine (2). Under an argon atmosphere, finely divided Me₃OBF₄ (3.40 g, 23.0 mmol) was added to a solution of 2-(isopropylamino)troponone (3.00 g, 18.4 mmol) in 20 mL of CH₂Cl₂. After stirring for 2 h, the golden solution was added dropwise over 30 min to

(16) Hilderbrand, S. A.; Lim, M. H.; Lippard, S. J. *J. Am. Chem. Soc.* **2004**, *126*, 4972–4978.

(17) Pangborn, A. B.; Giardello, M. A.; Grubbs, R. H.; Rosen, R. K.; Timmers, F. J. *Organometallics* **1996**, *15*, 1518–1520.

(18) Dias, H. V. R.; Jin, W.; Ratcliff, R. E. *Inorg. Chem.* **1995**, *34*, 6100–6105.

(19) Nolan, E. M.; Burdette, S. C.; Harvey, J. H.; Hilderbrand, S. A.; Lippard, S. J. *Inorg. Chem.* **2004**, *43*, 2624–2635.

(20) Lorković, I. M.; Ford, P. C. *Inorg. Chem.* **2000**, *39*, 632–633.

1,4-diaminobutane (6 mL, 60 mmol) and allowed to stir for an additional 2.5 h. The reaction was quenched by the addition of 20 mL H₂O and extracted with CH₂Cl₂ (3 × 50 mL). The solvent was removed under reduced pressure to yield a yellow oil. The crude product was dissolved in water with acidification to pH 3 with HCl. The solution was first extracted with CH₂Cl₂ to remove unwanted byproducts. The pH of the solution was then raised to 9 with aqueous NaOH followed by extraction with CH₂Cl₂ (3 × 50 mL). The organic extract was dried over MgSO₄ and filtered, and the solvent was removed under reduced pressure giving **6** (2.59 g, 60%) as a yellow oil. ¹H NMR (400 MHz, DMSO-*d*₆): δ 6.77–6.72 (2H, m), 6.32 (1H, d, *J* = 11.1 Hz), 6.26 (1H, d, *J* = 11.0 Hz), 6.12–6.07 (1H, m), 3.81 (1H, septet, *J* = 6.3 Hz), 3.25 (2H, t, *J* = 7.1 Hz), 2.57 (2H, t, *J* = 6.9 Hz), 1.65 (2H, p, *J* = 7.1 Hz), 1.44 (2H, p, *J* = 7.0 Hz), 1.17 (6H, d, *J* = 6.3 Hz). ¹³C NMR (100 MHz, DMSO-*d*₆): δ 152.1, 150.9, 133.0, 132.9, 117.2, 109.8, 45.7, 45.1, 41.5, 31.4, 27.0, 22.8. IR (NaCl, cm⁻¹): 3371 (w), 3217 (w br), 3022 (w), 2965 (m), 2929 (m), 2860 (w), 1609 (w), 1590 (s), 1538 (s), 1514 (s), 1464 (s), 1415 (m), 1384 (m), 1273 (m), 1207 (m), 1168 (m), 1122 (w), 974 (w), 952 (w), 882 (w), 863 (w), 845 (w), 818 (w), 745 (m br), 704 (m), 641 (w). HRMS (ESI) MH⁺: Calcd for C₁₄H₂₄N₃, 234.1970; Found, 234.1962.

H₂^{iPr}SATI-3 (3). Salicylaldehyde (157 mg, 1.29 mmol) in 5 mL of pentane was added to a solution of **1** (289 mg, 1.29 mmol) in 15 mL of pentane, and the reaction was stirred for 30 min. The pentane was decanted from the reaction flask to separate it from a small amount of brown oil that formed during the reaction. Removal of the pentane under reduced pressure afforded **3** as a yellow solid (370 mg, 89%). ¹H NMR (400 MHz, CD₂Cl₂): δ 8.38 (1H, s), 7.32–7.25 (2H, m), 6.93–6.85 (2H, m), 6.76–6.70 (2H, m), 6.40 (1H, d, *J* = 11.3 Hz), 6.20 (1H, d, *J* = 10.5 Hz), 6.12 (1H, t, *J* = 9.3 Hz), 3.86–3.75 (3H, m), 3.41 (2H, t, *J* = 6.7 Hz), 2.18 (2H, pentet, *J* = 6.4 Hz), 1.27 (6H, d, *J* = 6.3 Hz). ¹³C NMR (100 MHz, CD₂Cl₂): δ 165.65, 161.80, 154.13, 151.43, 133.84, 133.05, 132.48, 131.76, 119.46, 118.89, 117.96, 117.26, 113.88, 107.42, 58.14, 45.62, 45.29, 32.27, 22.97. IR (NaCl, cm⁻¹): 3213 (w br), 3062 (w), 2966 (m), 2927 (m), 2863 (m), 1632 (s), 1609 (m), 1589 (s), 1537 (s), 1510 (s), 1463 (s), 1414 (w), 1384 (m), 1276 (s), 1207 (m), 1167 (m), 1151 (w), 1119 (w), 975 (w), 952 (w), 882 (w), 845 (w), 755 (m), 704 (m), 640 (w). HRMS (ESI) MH⁺: Calcd for C₂₀H₂₆N₃O, 324.2076; Found, 324.2073.

H₂^{iPr}SATI-4 (4). To a solution of **2** (150 mg, 0.60 mmol) in 4 mL of CH₂Cl₂ was added salicylaldehyde (73 mg, 0.60 mmol) in 2 mL of CH₂Cl₂. After stirring overnight, the solvent was removed under reduced pressure yielding a golden-yellow oil that crystallized upon standing. The crystalline product was washed with cold hexanes to afford pure **4** (163 mg, 81%). ¹H NMR (400 MHz, DMSO-*d*₆): δ 8.38 (1H, s), 7.30–7.27 (2H, m), 6.93–6.88 (2H, m), 6.73–6.70 (2H, m), 6.34 (1H, d, *J* = 11.3 Hz), 6.24 (1H, d, *J* = 10.8 Hz), 6.12–6.09 (1H, m), 3.82 (1H, septet, *J* = 6.3 Hz), 3.67 (2H, t, *J* = 5.4 Hz), 3.36 (2H, t, *J* = 6.5 Hz), 1.88–1.82 (4H, m), 1.24 (6H, d, *J* = 6.3 Hz). ¹³C NMR (100 MHz, DMSO-*d*₆): δ 165.4, 161.8, 153.7, 151.6, 133.6, 133.0, 132.5, 131.7, 119.5, 118.9, 117.8, 117.3, 112.4, 108.5, 60.0, 47.4, 45.7, 29.5, 28.5, 23.0. IR (KBr, cm⁻¹): 3446 (w br), 3191 (w br), 3052 (w), 3027 (w), 2967 (w), 2917 (w), 2865 (w), 1629 (m), 1609 (w), 1589 (m), 1534 (m), 1509 (s), 1462 (m), 1383 (m), 1275 (m), 1205 (m), 1161 (w), 1150 (m), 1122 (w), 1083 (w), 1057 (w), 990 (w), 976 (w), 948 (w), 879 (w), 857 (w), 779 (w), 760 (m), 748 (m), 705 (m), 636 (w), 456 (w). HRMS (ESI) MH⁺: Calcd for C₂₁H₂₈N₃O, 338.2232; Found, 338.2213.

H₂^{iPr}FATI-3 (5). To a solution of 7'-chloro-4'-fluoresceincarboxaldehyde (90 mg, 0.23 mmol) in 100 mL of Et₂O was added **1**

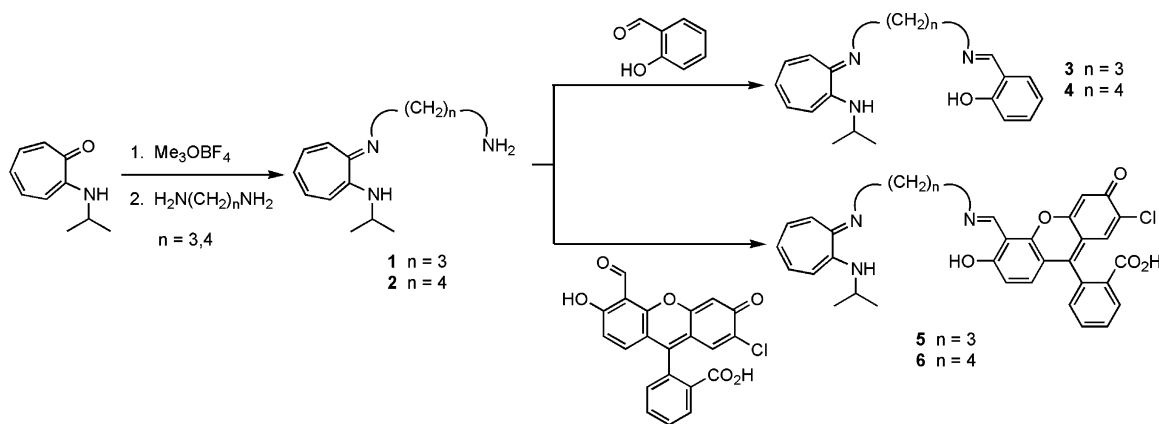
(50 mg, 0.23 mmol) in 8 mL of Et₂O. An orange precipitate formed immediately upon addition of 7'-chloro-4'-fluoresceincarboxaldehyde. After stirring for 30 min, the reaction was filtered, and the orange precipitate was dried in vacuo giving **5** (96 mg, 70%). ¹H NMR (400 MHz, DMSO-*d*₆): δ 9.10 (1H, s), 8.01 (1H, d, *J* = 7.5 Hz), 7.77–7.68 (2H, m), 7.27 (1H, d, *J* = 7.5 Hz), 6.89 (1H, s), 6.81–6.75 (2H, m), 6.69 (1H, s), 6.58 (1H, d, *J* = 9.2 Hz), 6.45 (1H, d, *J* = 11.5 Hz), 6.39 (1H, d, *J* = 9.3 Hz), 6.13 (1H, t, *J* = 9.2 Hz), 3.91–3.79 (3H, m), 3.42 (2H, t, *J* = 6.7 Hz), 2.11 (2H, p, *J* = 6.7 Hz), 1.20 (6H, d, *J* = 6.3 Hz). ¹³C NMR (100 MHz, DMSO-*d*₆): δ 173.10, 168.58, 160.46, 158.3, 152.91, 151.56, 150.79, 150.41, 148.9, 134.91, 134.08, 133.01, 130.18, 127.98, 125.73, 124.75, 119.13, 118.36, 114.28, 110.56, 108.72, 104.08, 103.89, 103.68, 51.88, 44.48, 44.28, 30.31, 22.06. IR (KBr, cm⁻¹): 3419 (w br), 3159 (w br), 2970 (w), 2923 (w), 1761 (m), 1644 (s), 1584 (s), 1517 (s), 1482 (s br), 1465 (s sh), 1440 (m sh), 1371 (s), 1343 (m sh), 1322 (m sh), 1277 (m), 1218 (m), 1169 (m), 1157 (m), 1093 (w), 997 (w), 884 (w), 830 (w), 762 (w), 703 (w), 667 (w), 627 (w), 595 (w), 549 (w), 470 (w). HRMS (ESI) MH⁺: Calcd for C₃₄H₃₁N₃O₅Cl, 596.1952; Found, 596.1957.

H₂^{iPr}FATI-4 (6). To a solution of 7'-chloro-4'-fluoresceincarboxaldehyde (80 mg, 0.20 mmol) in 8 mL of ethyl acetate was added **2** (53 mg, 0.23 mmol) in 2 mL of ethyl acetate. The solution containing a bright orange precipitate that formed was stirred for 30 min and filtered. The solid was washed with ethyl acetate and dried in vacuo, yielding **6** (79 mg, 65%) as a bright orange powder. ¹H NMR (400 MHz, DMSO-*d*₆): δ 9.12 (1H, s), 8.02 (1H, d, *J* = 7.5 Hz), 7.80–7.78 (2H, m), 7.29 (1H, d, *J* = 7.5 Hz), 6.90 (1H, s), 6.86–6.79 (2H, m), 6.70 (1H, s), 6.59 (1H, d, *J* = 9.3 Hz), 6.43 (1H, d, *J* = 11.4 Hz), 6.39 (1H, d, *J* = 9.3 Hz), 6.35 (1H, d, *J* = 11.0 Hz), 6.21–6.17 (1H, m), 6.10 (1H, m), 3.85–3.76 (3H, m), 3.34 (2H, d, *J* = 6.3 Hz), 1.80–1.73 (4H, m), 1.15 (6H, d, *J* = 6.2 Hz). ¹³C NMR (100 MHz DMSO-*d*₆): δ 173.16, 168.66, 160.37, 152.37, 152.13, 151.45, 150.56, 147.3, 134.61, 134.29, 134.15, 133.14, 130.04, 129.0, 127.86, 126.16, 125.19, 120.23, 119.09, 118.88, 112.87, 110.39, 110.05, 104.02, 103.88, 52.71, 45.57, 44.84, 28.00, 26.44, 21.71. IR (KBr, cm⁻¹): 3443 (w br), 3159 (w br), 3023 (w), 2970 (w), 2931 (w), 2865 (w), 1762 (m), 1643 (s), 1585 (s), 1516 (s), 1483 (s), 1465 (s sh), 1370 (s), 1275 (m), 1219 (m), 1169 (m), 1093 (w), 997 (w), 883 (w), 830 (w), 705 (w), 667 (w), 627 (w), 595 (w), 550 (w), 469 (w). HRMS (ESI) MH⁺: Calcd for C₃₅H₃₃N₃O₅Cl, 610.2108; Found, 610.2099.

[Co(^{iPr}SATI-3)] (7). Under an atmosphere of N₂, KH (480 mg, 12.0 mmol) was added to a solution of **3** (1.88 g, 5.8 mmol) in 40 mL of CH₃CN. An orange solution was obtained after stirring for 1 h. Upon addition of CoCl₂ (844 mg, 6.5 mmol) in 15 mL of CH₃CN over 15 min, the solution turned dark burgundy in color. After stirring for 3 h, the solvent was removed in vacuo. Crystallization from hot heptane afforded X-ray quality burgundy crystals of **7** (816 mg, 37%). IR (KBr, cm⁻¹): 2993 (w), 2960 (w), 2925 (w), 2835 (w), 2809 (w), 1602 (m), 1582 (m), 1535 (m), 1504 (m), 1471 (m), 1441 (m), 1405 (m), 1369 (m), 1351 (m), 1327 (m), 1275 (m), 1257 (w), 1228 (m), 1143 (m), 1127 (m), 1060 (m), 954 (w), 901 (w), 886 (w), 842 (w), 806 (w), 761 (w), 752 (m), 727 (m), 716 (m), 625 (w), 576 (w), 550 (w), 529 (w), 488 (w), 459 (w). Anal. Calcd for C₂₀H₂₃N₃OCo: C, 63.16; H, 6.10; N, 11.05. Found: C, 62.98; H, 6.16; N, 11.12.

[Co(NO)(^{iPr}SATI-3)] (8). Under an atmosphere of Ar, **7** (200 mg, 0.52 mmol) was dissolved in 10 mL of CH₂Cl₂ and exposed to excess NO. After stirring for 30 min, the solvent was removed in vacuo, and the resulting brown residue was washed with Et₂O and extracted into hot heptane. X-ray quality crystals of **8** (60 mg, 15%) were grown by slow evaporation of a solution of the crude

Scheme 2



product from heptane under an atmosphere of N_2 . IR (KBr, cm^{-1}): 2950 (w), 2919 (w), 2879 (w), 1639 (s), 1619 (s), 1587 (m), 1538 (w), 1504 (m), 1472 (m), 1455 (m), 1437 (m), 1412 (m), 1400 (m), 1333 (w), 1274 (w), 1230 (w), 1147 (w), 1067 (w), 959 (w), 912 (w), 889 (w), 871 (w), 844 (w), 758 (w), 737 (w), 724 (w), 715 (w), 612 (w), 481 (w), 462 (w), 437 (w). Anal. Calcd for $C_{20}H_{23}N_4O_2Co$: C, 58.54; H, 5.65; N, 13.65. Found: C, 58.77; H, 5.56; N, 13.92.

[Co₂(ⁱPrSATI-4)₂] (9). A portion of KH (12 mg, 0.30 mmol) was added to a 5 mL THF solution of **4** (50 mg, 0.15 mmol) under N_2 . An orange solution was obtained after stirring for 1 h. Addition of [Co(CH₃CN)₄](PF₆)₂ (92 mg, 0.18 mmol) in 10 mL of THF turned the solution dark burgundy. After stirring for 4 h, the solvent was removed in vacuo. The residue was extracted into CH₂Cl₂ and filtered through Celite. Pentane diffusion into a CHCl₃ solution of the complex gave X-ray quality crystals of **9** (39 mg, 66%). IR (KBr, cm^{-1}): 2958 (w), 2923 (w), 2862 (w), 1624 (m), 1593 (m), 1551 (w), 1510 (s), 1472 (m), 1445 (s), 1426 (m), 1412 (s), 1360 (m), 1331 (w), 1289 (m), 1263 (m), 1226 (m), 1149 (m), 1122 (w), 1011 (w), 987 (w), 853 (w), 886 (w), 857 (w), 817 (w), 783 (w), 758 (m), 719 (m), 669 (w), 588 (w), 568 (w), 463 (w), 443 (w). Anal. Calcd for $C_{42}H_{50}N_6O_2Co_2$: C, 63.96; H, 6.39; N, 10.65. Found: C, 63.86; H, 6.31; N, 10.68.

[Co(ⁱPrFATI-3)] (10). To a slurry of **5** (80 mg, 0.134 mmol) under an atmosphere of N_2 in 10 mL CH₃CN was added KH (11 mg, 0.275 mmol). After stirring for 1 h, [Co(CH₃CN)₄](PF₆)₂ (72 mg, 0.140 mmol) in 5 mL of CH₃CN was added. Continued stirring overnight afforded a dark red precipitate, which was filtered off and dried in vacuo to afford **10** (83 mg, 95%). IR (KBr, cm^{-1}): 3336 (w br), 3052 (w), 2963 (w), 2928 (w), 2870 (w), 1760 (m), 1633 (s sh), 1604 (s sh), 1575 (s), 1538 (s), 1503 (s), 1463 (s), 1397 (m), 1360 (m), 1339 (m), 1274 (w), 1221 (w), 1170 (m br), 1098 (w), 990 (m br), 885 (w), 827 (w), 761 (w), 716 (m), 630 (w), 591 (w), 551 (w), 480 (w), 467 (w). HRMS (ESI) M^+ : Calcd for $C_{34}H_{28}N_3O_5ClCo$, 652.1049; Found, 652.1046. Because of difficulties in the purification of **10**, it was not possible to obtain a satisfactory elemental analysis.

[Co(ⁱPrFATI-4)] (11). A 2 mL MeOH solution of NaOMe (600 μ L, 0.12 mmol of a 0.2 M solution in MeOH) was added to a 10 mL MeOH slurry of **6** (36.0 mg, 0.057 mmol) under N_2 . A clear, dark red-orange solution was obtained after stirring for 45 min. Upon addition of [Co(CH₃CN)₄](PF₆)₂ (29.0 mg, 0.057 mmol) in 5 mL of MeOH, the solution darkened. The reaction was allowed to stir for 5 h, and the solvent was removed in vacuo. The residue was extracted with 8 mL of acetone and filtered to leave **11** (29 mg) as a red-brown powder. IR (KBr, cm^{-1}): 3056 (w), 2956 (w), 2924 (w), 2861 (w), 1761 (w), 1709 (w), 1636 (m), 1608 (m), 1575 (s),

1537 (m), 1492 (m), 1465 (s), 1396 (s), 1338 (s), 1267 (m), 1228 (m), 1170 (m), 1096 (w), 1003 (m), 885 (w), 830 (w), 762 (w), 715 (w), 630 (w), 555 (w), 479 (w). HRMS (ESI) M^+ : Calcd for $C_{35}H_{30}N_3O_5ClCo$, 666.1206; Found, 666.1216. Because of difficulties in the purification of **11**, it was not possible to obtain a satisfactory elemental analysis.

X-ray Crystallography. Single crystals suitable for data collection were covered in Infineum V8512 oil (formerly called Paratone-N oil), mounted on the tips of glass capillary tubes, and transferred to a low-temperature nitrogen cold stream maintained by a Bruker KRYOFLEX BVT-AXS nitrogen cryostat. Data were collected on the Bruker diffractometer (Mo $K\alpha$ $\lambda = 0.71073$ Å) controlled by the SMART software package running on a Pentium II PC.²¹ The general procedures used for data collection are reported elsewhere.²² Empirical absorption corrections were calculated with the SADABS program.²³ Structures were solved by direct methods and refined with the SHELXTL and SAINTPLUS software packages on a Pentium II PC running the Windows NT operating system.^{24,25} All non-hydrogen atoms, unless otherwise noted, were refined anisotropically. Hydrogen atoms were assigned idealized positions and given a thermal parameter of 1.2 times the thermal parameter of the atom to which it was attached. All structure solutions were checked for higher symmetry with the program PLATON.²⁶

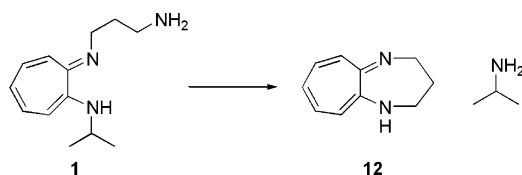
Complex **7** was solved in monoclinic $P2_1/c$. The β angle of approximately 90° suggested the possibility of higher symmetry or twinning whereby the unit cell is pseudo-orthorhombic. Attempts to model the twinning were made using the TWIN parameter in SHELXTL, but no suitable solution could be obtained. In addition, it was not possible to solve the structure using the higher symmetry orthorhombic cell by either direct or Patterson methods. The entire complex **7** is disordered over two positions and was modeled with 73.6% and 26.4% occupancies for the two orientations. It was not possible to refine anisotropically all atoms of the latter component.

Results and Discussion

Synthesis. The general synthetic route for the $H_2^{iPr}SATI-n$ and $H_2^{iPr}FATI-n$ ($n = 3, 4$) ligands is outlined in Scheme 2.

- (21) SMART: Software for the CCD Detector System, version 5.626; Bruker AXS: Madison, WI, 2000.
- (22) Kuzelka, J.; Mukhopadhyay, S.; Spingler, B.; Lippard, S. J. *Inorg. Chem.* **2004**, *43*, 1751–1761.
- (23) Sheldrick, G. M. *SADABS: Area-Detector Absorption Correction*; University of Göttingen: Göttingen, Germany, 2001.
- (24) SHELXTL: Program Library for Structure Solution and Molecular Graphics, version 6.2; Bruker AXS: Madison, WI, 2001.
- (25) SAINTPLUS: Software for the CCD Detector System, version 5.01; Bruker AXS: Madison, WI, 1998.
- (26) Spek, A. L. *PLATON, A Multipurpose Crystallographic Tool*; Utrecht University: Utrecht, The Netherlands, 2000.

Scheme 3



These molecules are constructed from the N,N' -disubstituted aminotroponimine class of ligands condensed either with salicylaldehyde or 7'-chloro-4'-fluoresceincarboxaldehyde. The isopropyl group on the aminotroponimine ring was chosen for ease of synthesis. A variety of other alkyl groups such as *t*-butyl, benzyl, and methyl were prepared with the related dansyl-aminotroponimine (H^R DATI) ligands,¹⁵ but there were no major differences among the metal complexes having these different alkyl groups.

The preparation of intermediates **1** and **2** was achieved by activation of 2-(isopropylamino)troponone with Me_3OBF_4 under argon followed by slow addition of the activated troponone to an excess of diamine. Intermediates **1** and **2** were then purified by selective precipitation and extraction from a dilute aqueous HCl solution after the pH was raised to 9 with NaOH, the yields being 33% and 60%, respectively. Compounds **1** and **2** are thermally sensitive yellow oils. On prolonged standing, even at $-80^\circ C$, **1** decomposed to a yellow solid, **12** (Scheme 3), identified by 1H NMR spectroscopy and comparison to literature data.²⁷ The condensations of **1** and **2** with salicylaldehyde afforded the salicylaldimines **3** and **4** in 80–90% yields. Ligands **3** and **4** are soluble in a variety of organic solvents including hexanes, Et_2O , CH_2Cl_2 , CH_3CN , and MeOH. Reaction of the appropriate aminotroponimine intermediate with 7'-

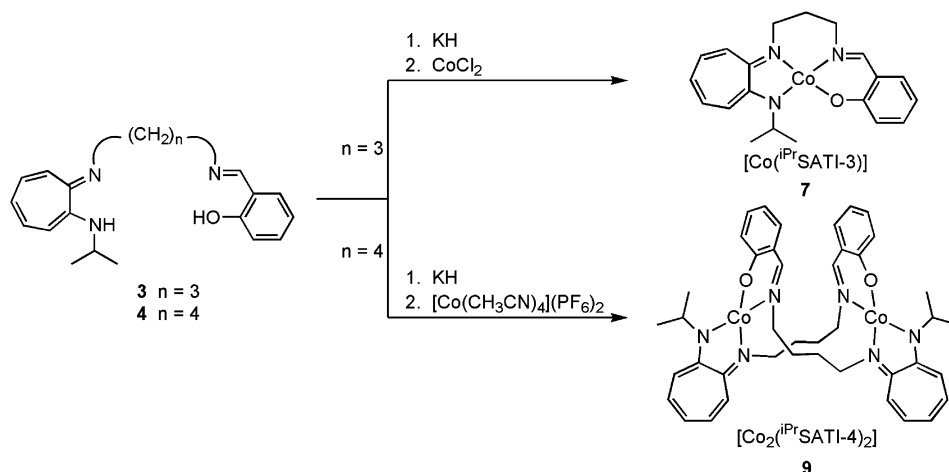
chloro-4'-fluoresceincarboxaldehyde in either $EtOAc$ or Et_2O cleanly and easily afforded **5** or **6** as bright orange powders, which precipitate from the reaction solution in 65–70% yields.

The metal complexes **7** and **9** were prepared by deprotonation of the ligand with 2 equiv of potassium hydride in THF or CH_3CN followed by addition of $[Co(CH_3CN)_4](PF_6)_2$ or $CoCl_2$ (Scheme 4). Complex **7** is mononuclear whereas **9** is dinuclear. In attempts to prepare mononuclear complexes with ligand **9**, bases such as sodium methoxide and sodium hydride were employed. The metalation reaction was also attempted in alternative solvents such as CH_2Cl_2 , CH_3CN , and MeOH; however, in all cases only dinuclear complexes were obtained. Both **7** and **9** are air-stable for several days as solids. The analogous H_2^{iPr} SATI-5 ligand, with an *n*-pentyl linker between the aminotroponimine and salicylaldimine groups, was also prepared, but it was not possible to isolate any metal complexes with this ligand. All metalation reactions with H_2^{iPr} SATI-5 produced intractable solids that had limited or no solubility in any of the solvents investigated, indicating possible oligomer formation. By admission of excess NO gas to a Schlenk flask containing **7**, the dark brown mononitrosyl **8** was formed. No nitrosyl products were isolated from the reaction of NO with **9**, however.

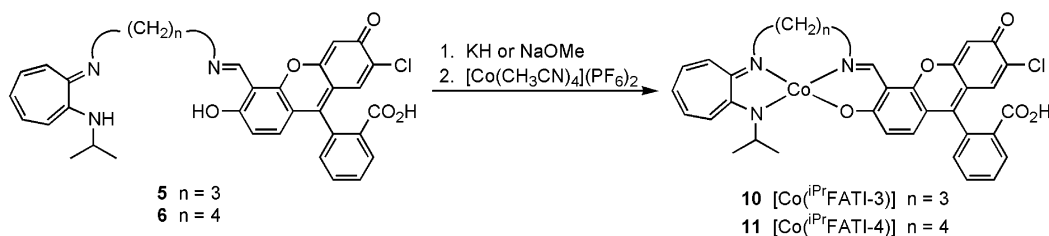
The fluorescein-containing complexes **10** and **11** were prepared by deprotonation of the respective ligand with either potassium hydride or sodium methoxide followed by addition of $[Co(CH_3CN)_4](PF_6)_2$ (Scheme 5). Purification of **10** and **11** was hindered by the inability to crystallize the products.

Structural Studies. The structures of complexes **7**, **8**, and **9** are displayed in Figures 1 and 2 as ORTEP diagrams, and X-ray crystallographic data for the complexes are given in

Scheme 4



Scheme 5



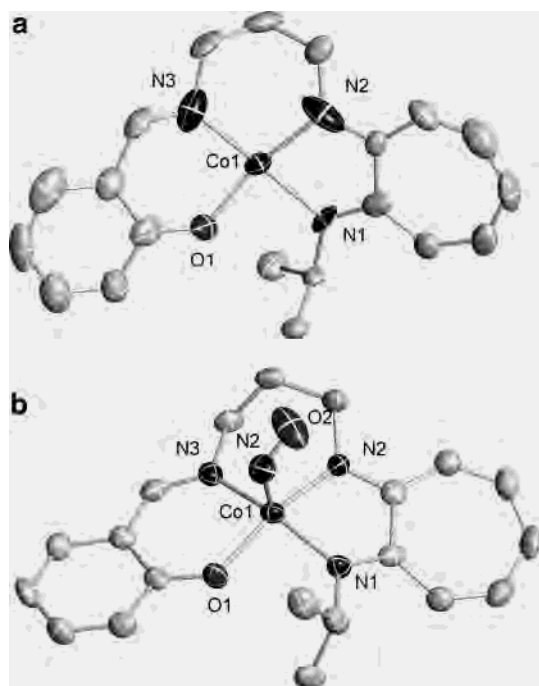


Figure 1. ORTEP diagrams of (a) $[\text{Co}(\text{iPrSATI-3})]$ (**7**) and (b) $[\text{Co}(\text{NO})(\text{iPrSATI-3})]$ (**8**) showing selected atom labels and 50% probability ellipsoids for all non-hydrogen atoms.

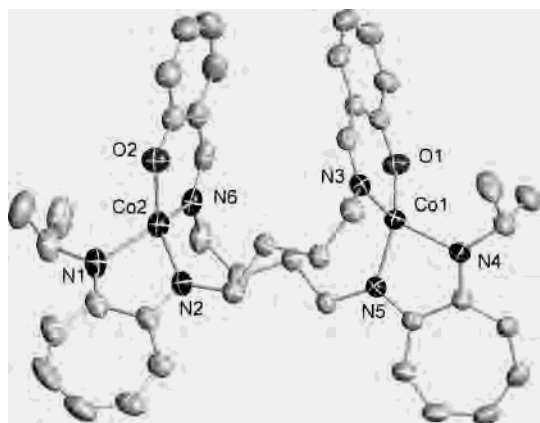


Figure 2. ORTEP diagram of $[\text{Co}_2(\text{iPrSATI-4})_2]$ (**9**) showing selected atom labels and 50% probability ellipsoids for all non-hydrogen atoms.

Table 1. Selected bond distances and angles from the single crystal X-ray diffraction data and those of related salicylaldimine^{28,29} and aminotroponimate³⁰ complexes are presented in Table 2. Complex **7** has a square planar geometry similar to those of $[\text{Co}(\text{salen})]$ and $[\text{Co}(\text{TC-3,3})]$ (Figure 3). The steric constraints imposed by the ethyl and propyl linkers in these ligands enforce a square-planar geometry, which is in contrast to the tetrahedral geometry common in many Co^{2+} complexes.³¹ The square planar geometry of **7** confers other

Table 1. Summary of X-ray Crystallographic Data for **7**, **8**, and **9**

	7	8	9 · CHCl_3 · C_5H_{12}
formula	$\text{C}_{20}\text{H}_{23}\text{N}_3\text{OCo}$	$\text{C}_{20}\text{H}_{23}\text{N}_4\text{O}_2\text{Co}$	$\text{C}_{48}\text{H}_{65}\text{N}_6\text{O}_2\text{Cl}_3\text{Co}_2$
fw	380.34	410.35	982.27
space group	$P2_1/c$	$P2_1/c$	$P2_1/n$
<i>a</i> , Å	9.351(1)	13.723(2)	13.8321(2)
<i>b</i> , Å	9.252(1)	14.452(2)	24.9517(1)
<i>c</i> , Å	20.722(3)	9.803(2)	14.6924(1)
β , deg	90.29(3)	109.674(3)	99.229(1)
<i>V</i> , Å ³	1792.8(4)	1830.6(5)	5005.21(8)
<i>Z</i>	4	4	4
ρ_{calc} , g/cm ³	1.409	1.489	1.304
<i>T</i> , °C	−100	−100	−100
$\mu(\text{Mo K}\alpha)$, mm ^{−1}	0.970	0.961	0.865
total no. of data	7888	14325	30866
no. of unique data	2586	4271	11459
no. of params	226	336	550
<i>R</i> ^a (%)	6.54	6.18	7.09
<i>wR</i> ^{2 b} (%)	16.33	12.57	15.15

$$^a R = \sum ||F_o| - F_c| / \sum |F_o|. \quad ^b wR^2 = \{ \sum [w(F_o^2 - F_c^2)^2] / \sum [w(F_o^2)^2] \}^{1/2}.$$

Table 2. Selected Bond Distances and Angles for **7**, **8**, and **9**^a

compd	distance	(Å)	angles	(deg)
7	Co1–N1	1.898(5)	N1–Co1–N2	83.4(3)
	Co1–N2	1.849(5)	N1–Co1–N3	176.9(2)
	Co1–N3	1.887(6)	N1–Co1–O1	90.1(2)
	Co1–O1	1.875(4)	N2–Co1–N3	96.6(3)
8	Co1–N1	1.914(3)	N1–Co1–N2	82.0(1)
	Co1–N2	1.904(3)	N1–Co1–N3	157.7(1)
	Co1–N3	1.954(4)	N1–Co1–N4	102.0(2)
	Co1–N4	1.807(4)	N1–Co1–O1	89.5(1)
	Co1–O1	1.903(3)	N2–Co1–N3	93.6(2)
	N4–O2	1.132(5)	N2–Co1–N4	96.7(2)
			N2–Co1–O1	166.5(1)
			N3–Co1–N4	100.3(2)
			N3–Co1–O1	90.4(1)
			N4–Co1–O1	95.2(2)
9	Co1–N3	1.984(3)	Co1–N4–O2	128.2(4)
	Co1–N4	1.970(3)	N1–Co2–N2	81.6(2)
	Co1–N5	1.955(3)	N1–Co2–N6	123.2(1)
	Co1–O1	1.904(3)	N1–Co2–O2	113.3(1)
	Co2–N1	1.978(4)	N2–Co2–N6	121.2(1)
	Co2–N2	1.968(3)	N2–Co2–O2	121.4(1)
	Co2–N6	1.993(3)	N6–Co2–O2	95.8(1)
	Co2–O2	1.908(3)	N3–Co1–N4	120.5(1)
			N3–Co1–N5	121.6(1)
			N3–Co1–O1	96.7(1)
$[\text{Co}(\text{salen})]^b$	Co–O _{salen}	1.852(5)		
	Co–N _{salen}	1.845(5)		
	Co–O _{salen(avg)}}	1.872(7)	Co–N–O _{avg}	127(1)
$[\text{Co}(\text{salen})(\text{NO})]^c$	Co–N _{salen(avg)}}	1.878(8)		
	Co–NO _{avg}	1.807(3)		
	N–O _{avg}	1.12(6)		
$[\text{Co}(\text{TC-3,3})]^d$	Co–N _{avg}	1.90(1)		
$[\text{Co}(\text{TC-3,3})\text{NO}]^e$	Co–N _{TC(avg)}}	1.90(1)	Co–N–O	127.3(6)
	Co–NO	1.785(6)		
	N–O	1.137(7)		

^a Numbers in parentheses are estimated standard deviations of the last significant figure. Atoms are labeled as indicated in Figures 1 and 2. ^b Reference 28. ^c Reference 29. ^d Reference 32. ^e Reference 30.

structural similarities to $[\text{Co}(\text{salen})]^{28}$ and $[\text{Co}(\text{TC-3,3})]^{32}$. The average Co–N distance from the aminotroponimate moiety of 1.874(6) Å in **7** is similar to the corresponding

(27) Nozoe, T.; Shindo, K.; Wakabayashi, H.; Ishikawa, S. *Heterocycles* **1992**, *34*, 881–884.

(28) Schaefer, W. P.; Marsh, R. E. *Acta Crystallogr., Sect. B* **1969**, *B25*, 1675–1682.

(29) Haller, K. J.; Enemark, J. H. *Acta Crystallogr., Sect. B* **1978**, *B34*, 102–109.

(30) Franz, K. J.; Doerrer, L. H.; Spingler, B.; Lippard, S. J. *Inorg. Chem.* **2001**, *40*, 3774–3780.

(31) Cotton, F. A.; Wilkinson, G. *Advanced Inorganic Chemistry*, 6th ed.; Wiley-Interscience: New York, 1999.

(32) Jaynes, B. S.; Doerrer, L. H.; Liu, S.; Lippard, S. J. *Inorg. Chem.* **1995**, *34*, 5735–5744.

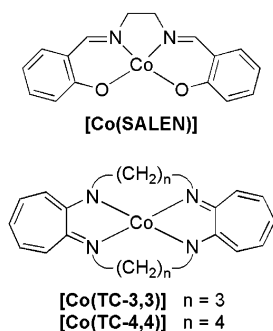


Figure 3. Structures of [Co(salen)], [Co(TC-3,3)], and [Co(TC-4,4)].

average of 1.90(1) Å in [Co(TC-3,3)].³² The Co–O and Co–N distances of 1.875(5) and 1.887(6) Å, respectively, are only slightly longer than the corresponding average distances of 1.852(5) and 1.845(5) Å, respectively, in [Co(salen)].²⁸

The dihedral angle Θ , measured between the planes of the salicylidiminate and aminotroponimate chelate rings, is 9.4° in **7**, indicating slight distortion from idealized square-planar geometry. The dihedral angle in **7** is similar to the corresponding angle of 9.0° observed in [Co(TC-3,3)], but larger than the Θ value of 2.2° in [Co(salen)].^{28,32} Another related but more flexible complex, [Co(TC-4,4)],³² has a Θ value of 32.0° and displays similar reactivity to **7**.

The mononitrosyl, **8**, is also structurally similar to the corresponding nitrosyl complexes of [Co(salen)] and [Co(TC-3,3)]. The nitrosyl N–O distance in **8** of 1.132(4) Å is comparable to the 1.12(6) Å average and 1.137(7) Å value from [Co(salen)NO] and [Co(TC-3,3)NO], respectively.^{29,30} The 1.807(4), 1.807(3), and 1.785(6) Å Co–NO distances in **8**, [Co(salen)(NO)], and [Co(TC-3,3)(NO)], respectively, are also quite similar. The Co–N–O angle of 128.2(4)° is in good agreement with the values reported for [Co(salen)(NO)] and [Co(TC-3,3)(NO)].^{29,30} Although **8** is structurally similar to [Co(salen)] and [Co(TC-3,3)], its reactivity in the presence of excess NO follows more closely that of [Co(TC-4,4)], *vide infra*.

Ligand **4** was designed to form mononuclear Co(II) complexes with a distorted tetrahedral geometry, as observed previously with [Co(ⁱPr-DATI)₂] and [Co(DATI-4)]. Instead, only dinuclear complexes were isolated. The two ligands in **9** bridge the Co(II) centers resulting in nearly tetrahedral geometries. The Θ values of 86.8° and 87.2° of the two metal centers in **9** are close to the 90° value for an idealized tetrahedron. These Θ values are very similar to the 89.5° Θ value reported for [Co(*i*-Pr₂ATI)₂], but much less constrained than the 63.3° Θ value for the mononuclear [Co(DATI-4)], which also has an *n*-butyl linker.¹⁵ The average Co–N bond distance of 1.968(3) Å in **9** is only slightly shorter than the value of 1.980(3) Å reported for [Co(*i*-Pr₂ATI)₂] and quite similar to the 1.970(5) Å value for [Co(TC-5,5)].^{15,32}

Although no X-ray structural data are available for **10** and **11** because of our inability to crystallize these complexes, related structures can be used to postulate their coordination geometry. Complex **10** is expected to have a square-planar geometry analogous to that of **7**. On the basis of the structural data for **9**, a similar dinuclear structure could be proposed

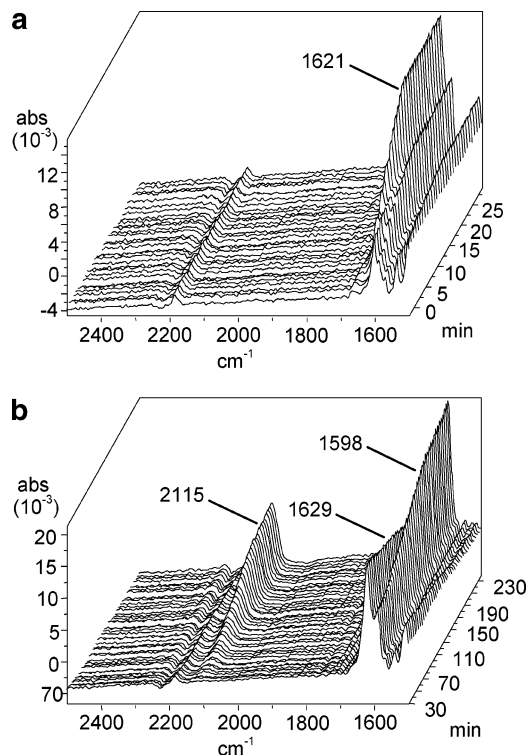


Figure 4. Solution IR spectra of [Co(ⁱPr-SATI-3)] (**7**) after exposure to excess NO in DMSO at room temperature: (a) 0–30 min exposure to NO and (b) 30–230 min after the addition of NO.

for **11**, although no evidence was observed in the APCI and high-resolution ESI mass spectral data to indicate the presence of a dinuclear species, which has an expected MH⁺ mass of 1334.3 amu. Given this result, a mononuclear complex with a distorted tetrahedral geometry similar to [Co(DATI-4)] seems more plausible, but the possibility of a dinuclear complex cannot be ruled out.

Reactivity. Figure 4 displays the solution IR spectra of an anaerobic DMSO solution of **7** following admission of excess NO at room temperature. The initial yellow-brown solution quickly turned dark red-brown within 10 min after exposure to NO. The first step in the reaction is formation of the crystallographically characterized mononitrosyl **8**, identified by its NO stretch at 1621 cm⁻¹. Within 40 min, additional IR features at 1598 and 2115 cm⁻¹ began to form. After 2.5 h, no additional spectral changes were observed. The IR band at 2115 cm⁻¹ is attributed to formation of a cobalt–dinitrogen species.³³ The related complex, [Co(TC-4,4)], also reacts similarly with formation of an IR band at 2108 cm⁻¹.³⁰ Isotope labeling experiments using ¹⁵NO previously conducted with [Co(TC-4,4)] indicated the presence of a dinitrogen adduct. The additional band that appears at 1598 cm⁻¹ in Figure 4 is consistent with the formation of a trigonal bipyramidal mononitrosyl complex similar to [Co(TC-4,4)(NO)], which has an NO stretch at 1584 cm⁻¹.³⁰ The initially formed mononitrosyl band at 1621 cm⁻¹ shifts to 1629 cm⁻¹ after approximately 30 min. Such a shift to higher energy was also observed in the disproportionation

(33) Chatt, J.; Dilworth, J. R.; Richards, R. L. *Chem. Rev.* **1978**, *78*, 589–625.

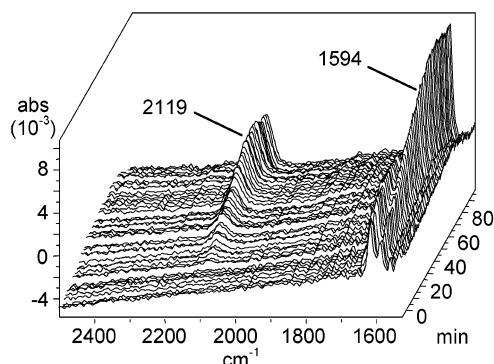


Figure 5. Solution IR spectra of $[\text{Co}_2(\text{iPrSATI-4})_2]$ (**9**) after exposure to excess NO in DMSO at room temperature.

reaction of $[\text{Fe}(\text{TC-5,5})]$ with NO.³⁴ In that reaction, NO₂ was formed and nitrated the tropolone rings of the ligand, creating a more electron-withdrawing ligand environment, and thus a higher energy nitrosyl stretch. With **7** there is no evidence for the formation of a $\text{Co}(\text{NO})_2$ species by IR spectroscopy, as occurs in the reactions of $[\text{Co}(\text{iPrDATI})_2]$ and $[\text{Co}(\text{DATI-4})]$ with NO, which would require dissociation of the salicylaldiminate or aminotroponimate fragment from the cobalt center.

Although **7** shares several structural similarities with $[\text{Co}(\text{salen})]$ and $[\text{Co}(\text{TC-3,3})]$, it is important to note that their reactivities with NO differ. Neither $[\text{Co}(\text{salen})]$ nor $[\text{Co}(\text{TC-3,3})]$ displays any further reactivity after formation of the mononitrosyl adducts. In fact, once formed, $[\text{Co}(\text{TC-3,3})\text{(NO)}]$ is stable enough that it can be recrystallized in air.³⁰ The difference in reactivity is interesting, since **7**, $[\text{Co}(\text{salen})]$, and $[\text{Co}(\text{TC-3,3})]$ all have similar Co–ligand bond lengths and Θ values less than 10° , which indicate nearly planar geometries. In contrast, the observed NO reactivity of $[\text{Co}(\text{TC-4,4})]$, which has a Θ value of 32.0° , is nearly identical to that observed for **7**. On the basis of these observations, we conclude that the differences in reactivity may be more a function of ligand flexibility than structural similarities at the cobalt center. Both **7** and $[\text{Co}(\text{TC-4,4})]$ should be more flexible than either $[\text{Co}(\text{salen})]$ or $[\text{Co}(\text{TC-3,3})]$. In the case of $[\text{Co}(\text{TC-3,3})]$, the two *n*-propyl linkers between the aminotroponimate rings severely limit the ability of the cobalt center to adopt new conformations. The *n*-butyl linkers in $[\text{Co}(\text{TC-4,4})]$ are more flexible and allow for formation of a trigonal bipyramidal mononitrosyl complex.³⁰ In **7**, the presence of only one *n*-propyl linker instead of the two present in $[\text{Co}(\text{TC-3,3})]$ should afford more flexibility.

The time-dependent solution IR spectra for the reaction of an argon-purged solution of **9** with excess NO at room temperature in DMSO are presented in Figure 5. During the course of the reaction, a single nitrosyl band grew in at 1594 cm^{-1} . This feature may correspond to a trigonal bipyramidal NO species, as postulated for the reaction of **7** and identified in the reaction of $[\text{Co}(\text{TC-4,4})]$ with excess NO. An additional IR band at 2119 cm^{-1} also began to form within the first 15 min of the reaction. Its appearance is significantly

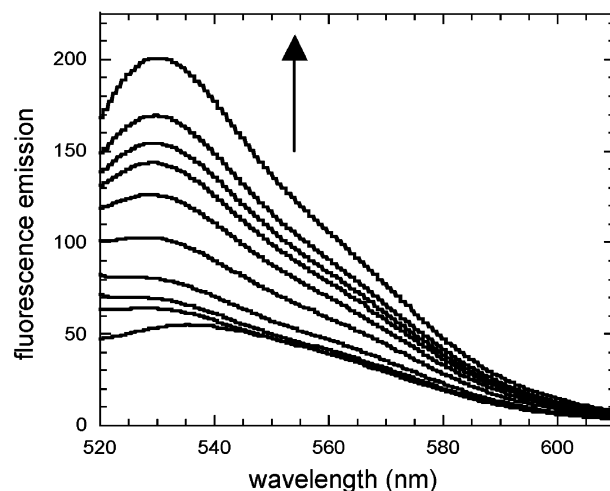


Figure 6. Fluorescence emission intensity spectra at 0 min, 5 min, 0.5 h, 1 h, 2 h, 4 h, 6 h, 8 h, 11 h, and 22 h following addition of excess NO to a $10\ \mu\text{M}$ solution of $[\text{Co}(\text{iPrFATI-4})]$ (**11**) in MeOH showing a 3-fold increase in fluorescence emission intensity. Excitation is at 503 nm and the emission maximum shifts from 535 nm before addition of NO to 530 nm after 22 h.

faster than in the reaction between **7** and NO, where the corresponding band at 2115 cm^{-1} was apparent only after 40 min. As with **7** and $[\text{Co}(\text{TC-4,4})]$, the IR band at 2119 cm^{-1} can be ascribed to formation of a cobalt–dinitrogen species. All attempts to isolate and characterize further such a putative dinitrogen adduct proved unsuccessful. When the solvent was removed from the reaction, however, the IR band at 2119 cm^{-1} was stable for several days in air. Although the possibility cannot be ruled out, there is no direct evidence for dissociation of the salicylaldiminate moiety of **9** from the cobalt center to form a dinitrosyl species.

The reaction of **10** with NO was followed by IR spectroscopy. Within 5 min after exposure of a solution of **10** in DMSO to excess NO, a new band that is consistent with a nitrosyl stretch appeared at 1630 cm^{-1} (Figure S1, Supporting Information), a result in good agreement with the nitrosyl band at 1621 cm^{-1} observed in the reaction of **7** with NO. Additionally, a second band began to appear at 2114 cm^{-1} 1 h after exposure to NO. Again, this feature is in good agreement with the results from **7**. As with **7**, no evidence was observed for formation of a dinitrosyl species; however, the intense band from the fluorescein carboxylic acid at 1759 cm^{-1} (Figure S1) may conceal bands from a dinitrosyl species.

Complex **11** reacted with excess NO in CH_3CN , displaying IR features similar to those observed for the reaction of **9** with NO. Following exposure to excess NO, a new band at 2117 cm^{-1} appeared. As with **7** and **10**, the 2117 cm^{-1} band corresponds to a possible dinitrogen adduct. An intense band at 1760 cm^{-1} , as expected, is consistent with either a lactone or carboxylic acid from the fluorescein.³⁵

Fluorescence Spectroscopic Measurements. The reaction of **10** with NO, when followed by fluorescence spectroscopy, did not exhibit a significant increase in fluorescence.

(34) Franz, K. J.; Lippard, S. J. *J. Am. Chem. Soc.* **1999**, *121*, 10504–10512.

(35) Silverstein, R. M.; Webster, F. X. *Spectrometric Identification of Organic Compounds*, 6th ed.; John Wiley and Sons: New York, 1998.

Exposure of **10** to excess NO in MeOH resulted in only a 20% increase in fluorescence emission intensity 4 h after exposure to NO (Figure S2, Supporting Information). If there were complete dissociation of the fluorescein moiety from the cobalt center, as observed with [Co(DATI-4)], a larger fluorescence increase, approaching that of the free ligand, would be expected. The absence of a large fluorescence increase, however, is not surprising because the solution IR data for the reaction do not indicate the formation of a dinitrosyl species, generation of which may result in fluorophore dissociation, as observed in the reaction of NO with [Co(^{iPr}DATI)₂].

A fluorescence study of **11** in MeOH showed a 3-fold increase in fluorescence 22 h after exposure to excess NO (Figure 6). This fluorescence response is similar to that previously observed for [Co(DATI-4)], but it is significantly slower. It is difficult to rationalize the fluorescence response of this system given the complex nature of the NO reactivity. The IR data exposed chemistry similar to that previously reported for [Co(TC-4,4)] with NO, where formation of several different species was apparent. In addition, the spectra revealed mononitrosyl and dinitrogen adducts. Because of the formation of multiple products, it is unclear which species gives rise to the increase in fluorescence intensity, the dinitrogen adduct, a mononitrosyl species, a potential dinitrosyl species, or another as yet unidentified product. On the basis of the small increase in fluorescence emission intensity observed on the reaction of **10** with NO, it seems unlikely that the fluorescence response of **11** results from the formation of the dinitrogen or mononitrosyl adducts, which are both revealed by solution IR spectral examination of the chemistry of **10**. Compound **11** is moderately stable to trace amounts of H₂O, although a 13% increase in fluorescence emission intensity occurred after addition of 10 μL of H₂O to a 10 μM solution of **11** in MeOH. The fluorescence emission intensity rapidly increased when **11** was dissolved in pH 7.4 phosphate buffer, however. A 2.5-fold increase in emission intensity was recorded between 10 min and 3 h after preparation of the buffer solution (Figure S3, Supporting Information). The fluorescence increase in aqueous solution is presumably due to dissociation of the metal complex to afford the free ligand. Although **10** and **11** are sufficiently air stable in solution, the complicated slow reactivity with

NO and sensitivity to water limits the potential uses of this system for measuring of NO in aqueous environments.

Conclusions

A new series of ligands containing an aminotroponimine moiety linked by an alkyl chain to a salicylaldimine or a fluorescein have been prepared, and their coordination chemistry has been investigated. The Co(II) complexes of the salicylaldimine ligands, **7** and **8**, were prepared and structurally characterized. Complex **7** reacts with NO to form an initial mononitrosyl species, which then undergoes further reactivity in the presence of excess NO to form a dinitrogen adduct, as characterized by solution IR spectroscopy. The reactivity of **7** is similar to that of [Co(TC-4,4)]. Complex **9**, formed by the reaction of [Co(CH₃CN)₄](PF₆)₂ with ligand **4**, gives a dinuclear species in which the two ligands bridge the two cobalt centers. It also reacts with NO ultimately to form a dinitrogen adduct. This chemistry was extended to complexes utilizing a derivatized fluorescein ligand fragment. Although no X-ray crystallographic characterization of **10** and **11** was possible, mass spectrometric data indicate both complexes to be mononuclear; in the case of **11**, a dinuclear structure similar to **9** cannot be ruled out. As expected, the NO reactivity of **10** and **11** is similar to that observed for the model complexes **7** and **9**. A modest, but slow, 3-fold increase in fluorescence emission intensity is observed 22 h after exposure of **11** to excess NO. Because multiple products form during the reaction, none of which could be crystallized, it is unclear what species gives rise to the increase in fluorescence emission intensity. It is unlikely that the increase in emission intensity is from the mononitrosyl or dinitrogen adducts, since only minimal fluorescence response was observed following exposure of **10** to NO, where both the dinitrogen and mononitrosyl adducts are apparent.

Acknowledgment. This work was supported by NSF Grant CHE-0234951. The MIT DCIF NMR spectrometer was funded through NSF Grant CHE-9808061.

Supporting Information Available: Figures S1 and S2 for the reaction of **10** with NO monitored by IR spectroscopy and the fluorescence response of **11** in aqueous buffer, and X-ray crystallographic files (CIF). This material is available free of charge via the Internet at <http://pubs.acs.org>.

IC049776H